ChemComm

Accepted Manuscript

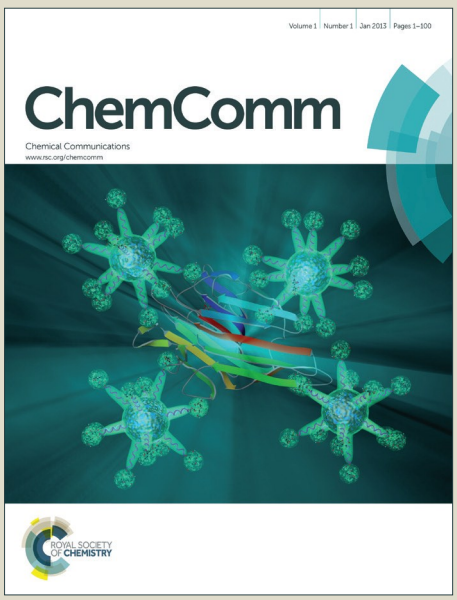

ROYAL SOCIETY OF CHEMISTRY

www.rsc.org/chemcomm

Journal Name

RSCPublishing

COMMUNICATION

DNA Strand Displacement Reaction for Programmable Release of Biomolecules

Cite this: DOI: 10.1039/xoxxoooooox

Hamid Ramezani[a] and D. Jed Harrison[b]

Received ooth January 2012,
Accepted ooth January 2012

DOI: 10.1039/xoxxoooooox

www.rsc.org/

Sample cleanup is a major processing step in many analytical assays. Here, we propose an approach to capture-and-release of analytes based on the DNA strand displacement reaction (SDR) and demonstrate its application to a fluoroimmunoassay on beads for a thyroid cancer biomarker, thyroglobulin. The SDR-based cleanup showed no interference from matrix molecules in serum.

The non-specific adsorption of matrix macromolecules in biological samples on solid supports often poses a big challenge to the accuracy and proficiency of assays through matrix effects.[1] Increased noise levels[2] and interferences with the analyte signal are common as a result.[3] Besides employing non-fouling surfaces,[1b,2] it can be effective to employ sample cleanup steps prior to quantification.[1a] One straightforward cleanup method is the specific capture and subsequent release of an analyte, for instance in solid phase extraction, or when using antibody-functionalized magnetic beads.[4] However, the significant change in solvent or thermal conditions required for release means that many techniques still suffer from interference by matrix molecules, as they may also be released by the changed conditions. A methodology that is highly specific binding and release, that does not require changed conditions (such as pH or ionic strength[5]) would be advantageous. Here, we exploit DNA hybridization, followed by a strand displacement reaction (SDR)[6] as a very specific and programmable capture-and-release tool, which does not require changing buffer conditions. Instead, the specific release is achieved via SDR, a concept used in DNA biomolecular chemistry that provides rapid, isothermal dehybridization.

SDR[6] is one of the commonly used techniques in DNA nanotechnology[7] and molecular beacon-based sensing.[8] In the displacement reaction, two DNA single strands both complementary to the same template are used sequentially. The DNA strand with the larger number of matched nucleobases (also called a fuel strand) will replace the other strand already duplexed to the template,[6,9] driven by forming a more thermodynamically stable duplex (Scheme 1a). The nucleation site for the fuel on the template strand is sometimes referred to as the "toehold".[9] The SDR is a fast, efficient, specific, and isothermal reaction and all these features are favorable in a sample cleanup technique.

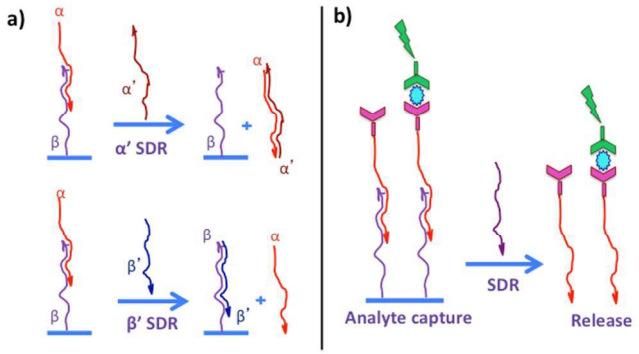

Scheme 1 a) Two possible ways of releasing the α capture strand off the surface using SDR: for the top series α bears the toehold and is released by fuel strand α' as a duplex while for the bottom series, β contains the toehold sequence and α is released by β' as a single strand. b) SDR-driven release combined with fluoroimmunoassay: the *in situ* cleanup relies on DNA-directed immobilization for the capture of sandwich complex and SDR for the subsequent release back into a buffer. Specific release of the captured molecules is triggered by addition of the sequence-encoded fuel strand, without any change in buffer properties or temperature.

Fluoroimmunosorbent assays (FIA)[10] are well-established techniques in bioanalytical chemistry. They are often negatively influenced by the sample matrix[11] and the background noise arising on a solid support.[12] A highly specific release step incorporated into the assay, so that the signal could be read in a solution ideally free of matrix molecules, would improve performance. Herein, we first demonstrated that the SDR-mediated release scheme works effectively on silica microparticles functionalized with a relevant DNA probe. A monoclonal antibody was then conjugated[13] to a capture DNA strand, α, giving an α-Ab conjugate. This conjugate

was immobilized on beads through duplex formation between the capture and probe strands. An antibody-antigen-labeled antibody sandwich complex was subsequently formed on the bead. The complex was then released from the beads using a SDR and was quantified in solution by fluorescence spectroscopy (Scheme 1b). The purpose of this study is to introduce use of the SDR process as a highly selective capture and release tool.

We selected a thyroid cancer biomarker, thyroglobulin (Tg),[14] immunoassay as the model to demonstrate the use of SDR for specific release of an immunosorbed complex. Besides its clinical importance, thyroglobulin is a huge multimeric protein (MW 660 kDa) making it a challenging model antigen for the current study. Tg shows significant non-specific adsorption, slow mass transfer, and is determined in serum, a complex sample matrix. The SDR was integrated into a sandwich FIA for thyroglobulin (Tg)[14], as illustrated in Scheme 1b.

To demonstrate that the SDR on beads is fast and efficient, the 2 μm carboxylated silica beads were first functionalized with neutravidin through the standard EDC/NHS chemistry.[15] The biotinylated probes were then fixed on the beads using the strong biotin-avidin interaction.[16] They were either partially complementary (β) or non-complementary (Ctrl) to the capture strand. The capture strand, α, labeled with carboxyfluorescein (FAM) was captured on 1.5 mg of beads in a hybridization step, followed by three washes. Finally, an incubation with the fuel strand, β', released the captured α strand via SDR. At the end of each step, the beads were pelleted by centrifugation and the supernatants were analyzed by fluorimetry. The beads were re-suspended at the beginning of each step using a bench-top vortex.

The SDR on beads happens fairly fast, with a high efficiency (90% when β' is the fuel strand), as indicated in Fig. 1. The reproducibility of the process is very good and the RSD values for β' SDR capture and release are 2.8% and 5.6%, respectively. There is no detectable release off the control beads (Fig. 1). These findings confirm the specific nature of the DNA sequence-mediated capture and release.

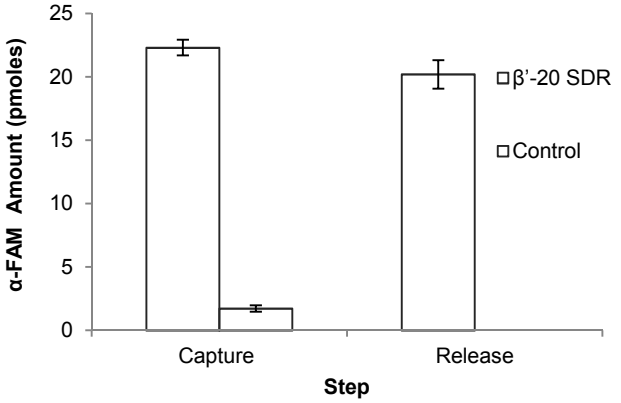

Fig. 1 Proof of concept of SDR-mediated release on beads. The amounts of α-FAM (on y axis) were calculated based on its concentrations in the supernatants at the ends of both capture and release steps (on x axis). The captured amount in the control experiment was because of non-specific adsorption of α-FAM.

To integrate the SDR-mediated release with an immunofluorometric assay on beads, the primary antibody should be conjugated to the capture strand, α. The steps needed to do such an assay include DNA-directed immobilization[17] of the primary antibody on the beads, incubation of the antigen, then the labeled secondary antibody, and eventually release via hybridization of the fuel strand (Scheme 1b). Surface Plasmon Resonance (SPR) spectrometry[18] was used to analyze the binding interactions, providing real time imaging of the binding events, and insights into the effects of non-specific adsorptions and steric hindrance on the SDR-mediated release of the complex. On a Biacore chip bearing the biotinylated β probes the α-TgAb conjugate was immobilized and the antigen (human Tg) and the secondary antibody (TgAb-FAM) were subsequently added to form the immunosorbed sandwich complex. The chip was then exposed to the fuel strand α'-25, yielding 48% release of the sandwich complex (Table 1, compiled based on the sensogram shown in Supplementary Fig. S2). The data in Table 1 demonstrates that each of the assay steps occurs as expected. Notably, a prior surface passivation with bovine serum albumin (BSA) was necessary. SPR traces showed that BSA treatment significantly improved the SDR yield, by suppressing non-specific adsorption of the α-TgAb conjugate, Tg, and TgAb-FAM. We also noted the SDR yield for removal of the α-TgAb conjugate (MW ~ 160 kDa) alone was about 88%, in contrast to 48% release for the sandwich complex (MW ~ 970 kDa). This drop in SDR yield may arise from reduced accessibility of the toehold for α'-25 in the presence of the sandwich complex, or from avidity,[19] arising from multivalent TgAb-Tg binding. While the antibody:DNA ratio was tuned to be around 1, avidity is still possible when TgAb bridges the adjacent Tg antigens at higher α-TgAb conjugate densities. Tg is a huge, multimeric protein and is very likely to display multiple copies of the same epitope on each molecule, resulting in significant avidity.

Step	Signal change in RU (experiment)	Signal change in RU (control)
BSA	- 5	7
α-TgAb conjugate	2902	2941
BSA	- 9	- 9
Tg	1535	No injection
BSA	- 9	No injection
TgAb-FAM	410	- 1
α'-25 fuel	-2334	- 2575
Total capture	4824	2938
α'-25 SDR yield (%)	**48.4**	**87.6**

Table 1 SPR was used to monitor each step of sandwich complex formation and SDR-mediated release. SPR signal level changes in RU (resonance unit) were calculated by subtracting the signal level before the injection from the one after the injection, after the signal was stable. A negative value for the signal level change means the signal dropped by that amount. All injections were at 5.0 μL/min and the injection volume of 15.0 μL. For more details refer to Table S1 and Fig. S2. The α'-25 SDR yields were obtained by dividing the signal drop due to the injection of α'-25 by the total capture signal.

A second SPR study was used to estimate the optimal concentration of the fuel strand. A fixed concentration of α was first captured on a β-functionalized chip and was subsequently released using different concentrations of α'-25 fuel. The results showed that above a stoichiometric ratio of α' to α, the displacement efficiency did not change substantially. The SDR yields for the α release increased only 2% and 4%, respectively, for a 2 x or 9 x excess concentration of fuel strand. (see Supplementary Fig. S1). We, therefore, used fuel concentrations larger than at least 5 times the corresponding concentration of α in each bead experiment.

The surface density of primary antibody on beads is a potentially important factor in the assay performance, and is governed by the concentration of the capture agent, α-TgAb conjugate, during surface loading with the conjugate plus the surface densities of β probes and neutravidin. Choosing too low a conjugate concentration or β probe density sacrifices the assay sensitivity. The β probe density was set so that the SDR-mediated release of α-FAM would generate a signal in the middle of the linear range of the α-FAM calibration curve. To optimize performance, we examined the capture and release profiles

for the sandwich complex (α-TgAb/Tg/TgAb-FAM) as a function of different concentrations of the conjugate during surface loading. The sandwich complex release efficiency decreases significantly when the surface of the beads is overcrowded with conjugate; that is when conjugate is loaded on the beads at concentrations above 40 μg/mL (Fig. 2). This may be due to the decreased accessibility of the toeholds on the probes to the fuel strand, or to more cooperativity in antibody-antigen binding (avidity).[19] It is important to select a conjugate concentration that gives rise to the optimal density of conjugates on the surface. Fig. 2 shows that a solution concentration range of 10-40 μg/mL for the conjugate results in the highest release yield for the sandwich complex. (Fig. S3 includes the capture and release profiles used to prepare Fig. 2).

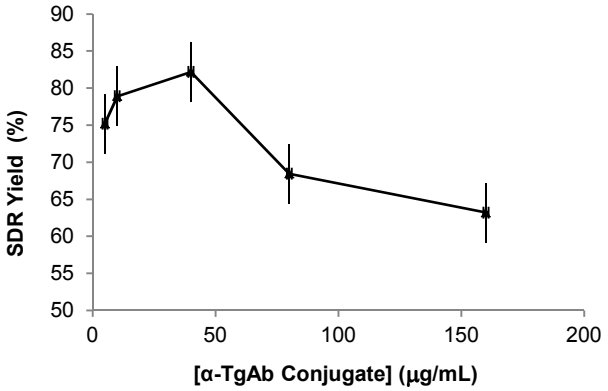

Fig. 2 DNA-directed immobilization of the conjugate on the beads makes its solution concentration dictate its surface density. The conjugate surface density, in turn, influences the release yields in SDR-mediated FIA of a fixed concentration of Tg. The highest SDR yields of release lie in the α-TgAb conjugate concentration range of 10-40 μg/mL.

Ideally, the release yield should be independent of the concentration of antigen for a fixed surface loading concentration of the conjugate. To calculate the SDR release efficiencies, calibration curves for the capture and release of Tg were obtained (Fig. 3, black curves corresponding to the left vertical axis in AFU). The capture curve and the release curve do not show a big difference in the saturation concentrations at which they reach their plateaus (Fig. 3) (Supplementary Fig. S4 examines the linear ranges of capture and release profiles shown in Fig. 3). This is consistent with the assumption that at a fixed solution concentration of the conjugate, its surface density has remained the same for all different concentrations of the antigen. In agreement with the results obtained from SPR, the SDR yield on beads for the labeled unconjugated α strand (90%) is larger than for the sandwich complex (63-82%) on beads.

As expected, the release to capture signal ratios stay almost constant at different concentrations of the antigen, although there is some difference at lower antigen concentrations (Fig. 3, blue curve corresponding to the right vertical axis in percentage). The non-specific portion of capture constitutes a significant fraction of the total capture signal at the lowest concentrations, leading to underestimation of the signal ratios at the low end. The term "signal ratio" was used instead of the SDR yield because the non-specific capture was not subtracted from the total capture in this data set.

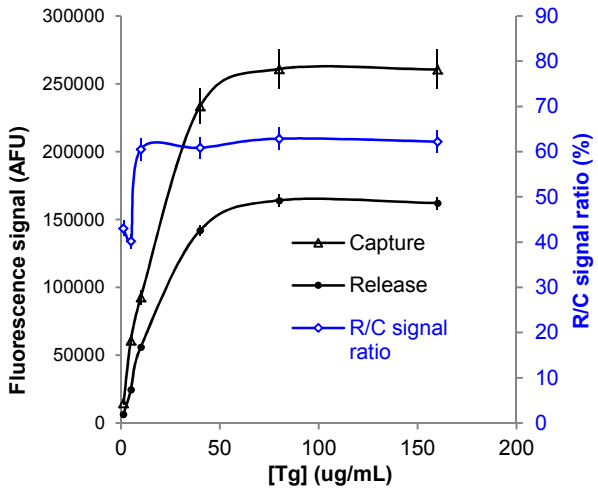

Fig. 3 Capture and release profiles of the antigen, Tg, at the fix [α-TgAb] of 40 μg/mL (black curves) were used to estimate the release to capture (R/C) signal ratios (blue curve). The R/C signal ratios stay almost constant when the conjugate density on the surface is kept the same (blue curve corresponding to the right vertical axis) because the SDR yield remains constant.

The calibration curves for Tg in both buffer and serum, determined across a Tg concentration range relevant to clinical chemistry (above 2 ng/mL to μg/mL[20]), are shown in Fig. 4. The presence of the complex matrix molecules clearly has no significant negative effect on the performance of the assay in serum. The linear range for the Tg detection is 12.6-2000 ng/mL for Tg in the serum (R^2= 0.998) (Fig. 4). Since slightly different solution concentrations of the α-TgAb conjugate during bead surface loading were used, the release fluorescent signal intensities (Fig. S5) were normalized with respect to the conjugate concentration (20.0 μg/mL in case of buffer and 22.6 μg/mL for the spiked serum) in Fig. 4.

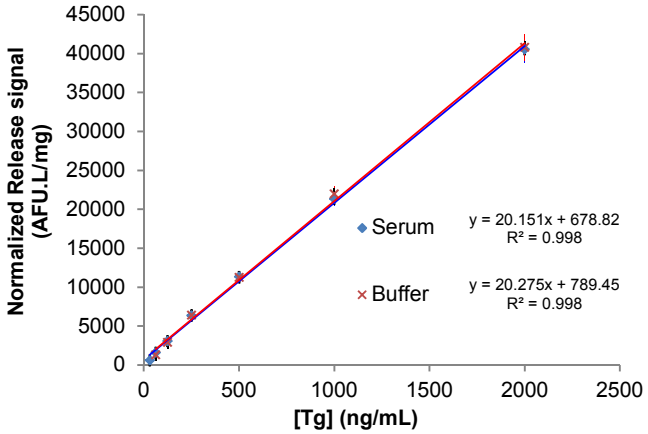

Fig. 4 The normalized calibration curve for Tg captured from spiked serum samples and released into a buffer shows a performance similar to the Tg in buffer samples. The two calibration curves are almost on top of one another (see Fig. S6). This means that the SDR-based cleanup can successfully remove the possible matrix interferences.

The typical RSD of release for the triplicate measurements of a Tg concentration (62.5 ng/mL) in the lower end of the spiked serum calibration curve was 4.2%.

It is also worth mentioning that the dynamic range of the assay could be shifted to a desired concentration range by changing the

experimental conditions. This is evident from comparing Fig. 4 with Fig. S4, where changing the conjugate concentration and instrumental sensitivity led to a shift in dynamic range toward much less Tg concentrations.

It was also observed that similar release efficiency was achievable with α'-25 as the fuel strand instead of β'-20 (Fig. 5 and Fig. S7). This indicates that the position of toehold does not cause a significant change in release yields, at least at the concentrations of antigen and fuel strand employed in this study.

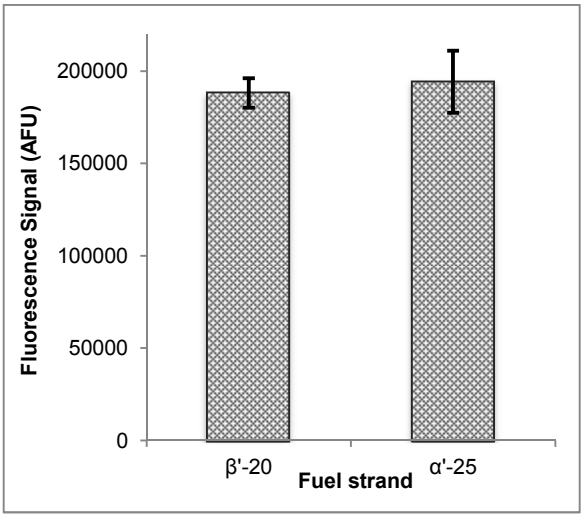

Fig. 5 Effect of fuel strand type on the release signal at the Tg concentration of 62.5 ng/mL in serum. No significant difference was observed no matter where the toehold is located, on the β probes much closer to the beads surface or on α farther away from the surface but very close to the Ab-Ag sandwich complex.

Conclusions

We demonstrated the successful application of the DNA strand displacement reaction (SDR) to the sequential capture and release of an antigen, thyroglobulin, and its sandwich antibody complex. Addition of such a fast, efficient, and *in situ* cleanup mechanism to a conventional fluoroimmunosorbent sandwich assay on beads will provide an additional aid in overcoming non-specific adsorption. This sort of capture and release tool could potentially be integrated into other assay formats. It also lends itself to multiplexing given the sequence-specific nature of the DNA duplex formation.

Notes and references

[a,b] Department of Chemistry, University of Alberta, 11227 Saskatchewan Drive NW, Edmonton, AB, Canada T6G 2G2

E-mail: Jed.Harrison@ualberta.ca

Homepage: http://www.chem.ualberta.ca/~harrison/.

† This work was supported by the Natural Sciences and Engineering Research Council of Canada (NSERC) and National Institute for Nanotechnology (NINT).

Electronic Supplementary Information (ESI) available. See DOI: 10.1039/c000000x/

1 (a) C. Nistor and J. Emnéus, in *Comprehensive analytical chemistry*, ed. L. Gorton, Elsevier, 2005, pp. 375-427; (b) P. Gong and D. W. Grainger, *Methods Mol Biol*, 2007, **381**, 59.

2 A. Hucknall, S. Rangarajan and A. Chilkoti, *Adv. Mater.*, 2009, **21**, 2441.

3 J. Tate and G. Ward, *Clin Biochem Rev*, 2004, **25**, 105.

4 T. Lea, F. Vartdal, K. Nustad, S. Funderud, A. Berge, T. Ellingsen, R. Schmid, P. Stenstad and J. Ugelstad, *J Mol Recognit*, 1988, **1**, 9.

5 R. Burgess and N. Thompson, *Curr. Opin. Biotechnol.*, 2002, **13**, 304.

6 D. Zhang and G. Seelig, *Nat Chem*, 2011, **3**, 103.

7 N. C. Seeman, *Angew. Chem. Int. Ed.*, 1998, **37**, 3220.

8 (a) S. Tyagi and F. Kramer, *Nat. Biotechnol.*, 1996, **14**, 303; (b) Q. Li, G. Luan, Q. Guo and J. Liang, *Nucleic Acids Res.*, 2002, **30**, e5.

9 D. Zhang and E. Winfree, *J. Am. Chem. Soc.*, 2009, **131**, 17303.

10 I. Hemmila, *Clin. Chem.*, 1985, **31**, 359.

11 (a) E. Ishikawa, S. Hashida and T. Kohno, *Mol. Cell. Probes*, 1991, **5**, 81; (b) L. J. Kricka, *Clin. Chem.*, 2000, **46**, 1037.

12 M. Seydack and U. Reschgenger, in *Standardization and quality assurance in fluorescence measurements ii: Bioanalytical and biomedical applications*, 2008, pp. 401-428.

13 (a) C. Niemeyer, T. Sano, C. Smith and C. Cantor, *Nucleic Acids Res.*, 1994, **22**, 5530; (b) J. Ladd, A. Taylor, M. Piliarik, J. Homola and S. Jiang, *Anal. Chem.*, 2008, **80**, 4231.

14 (a) A. Carpi, J. Mechanick, S. Saussez and A. Nicolini, *J. Cell. Physiol.*, 2010, **224**, 612; (b) C. F. Eustatia-Rutten, J. W. Smit, J. A. Romijn, E. P. Van Der Kleij-Corssmit, A. M. Pereira, M. P. Stokkel and J. Kievit, *Clin Endocrinol*, 2004, **61**, 61.

15 (a) G. Cline and S. Hanna, *J. Org. Chem.*, 1988, **53**, 3583; (b) D. Sehgal and I. Vijay, *Anal. Biochem.*, 1994, **218**, 87.

16 (a) E. Diamandis and T. Christopoulos, *Clin. Chem.*, 1991, **37**, 625; (b) P. C. Weber, D. H. Ohlendorf and J. J. Wendoloski, *Science*, 1989, **243**, 85.

17 (a) C. M. Niemeyer, *Trends Biotechnol.*, 2002, **20**, 395; (b) C. Zhang, C. Tian, F. Guo, Z. Liu, W. Jiang and C. Mao, *Angew. Chem. Int. Ed. Engl.*, 2012, **51**, 3382.

18 (a) B. Liedberg, I. Lundstrom and E. Stenberg, *Sens. Actuators, B*, 1993, **11**, 63; (b) B. P. Nelson, T. E. Grimsrud, M. R. Liles, R. M. Goodman and R. M. Corn, *Anal. Chem.*, 2001, **73**, 1.

19 (a) G. Vauquelin and S. Charlton, *Br. J. Pharmacol.*, 2013, **168**, 1771; (b) M. Mammen, S. Choi and G. Whitesides, *Angew. Chem. Int. Ed.*, 1998, **37**, 2755; (c) V. Mani, D. P. Wasalathanthri, A. A. Joshi, C. V. Kumar and J. F. Rusling, *Anal. Chem.*, 2012, **84**, 10485.

20 (a) L. Giovanella, *Clin. Chem. Lab. Med.*, 2008, **46**, 1067; (b) A. Iervasi, G. Iervasi, M. Ferdeghini, C. Solimeo, A. Bottoni, L. Rossi, C. Colato and G. Zucchelli, *Clin Endocrinol*, 2007, **67**, 434.

